Power Quality Improvement in a Fuel-Cell Based Micro-Grid with Shunt Active Power Filter

Niranjan Nayak*, Devi Prasad Acharya**‡, Subhashree Choudhury***, Rohan Padhy****

* Department of EEE, ITER, Professor, SOA Deemed to be University, ITER

**Department of EEE, Research Scholar, SOA Deemed to be University, ITER

***Department of EEE, Associate Professor, SOA Deemed to be University, ITER

****Department of EEE, B.tech Student, SOA Deemed to be University, ITER

(niranjannayak@soa.ac.in, deviprasad049@gmail.com, subhashreechoudhury@soa.ac.in, padhyrohan71@gmail.com)

‡ Devi Prasad Acharya, 751019, Tel: +90 8328953908, deviprasad049@gmail.com

Received: 27.03.2020 Accepted:01.05.2020

Abstract- The rapid industrial growth and population increase is the cause of production of abundant power, which is necessary in modern scenario. The factors like reliability of power, maintenance of power quality, increased efficiency of power sources are the new challenges in front of power Engineers. The tremendous scarcity of conventional power leads to alternate nonconventional energy sources. The most suitable alternate source of energy is solar power which has few drawbacks such as partial shading effects and interruption of power in rainy season and at night time, intermittent and nonlinear nature etc. The alternate energy plays key role due to its green and clean nature of production, easy availability and free from air pollution. Exploration of alternative fuel type leads to the efficient use of renewable energy sources with more distributed generation. For this purpose, micro grid with distributed generation plays a pivotal part in fulfilling the desired objectives during dispersal of energy. This paper provides the efficient operation of a fuel cell stack supplying a nonlinear load connected to grid. The operation is optimized by the employment of an Active power filter connected parallel (SAPF) at the Point of Common Coupling (PCC). The power quality is maintained by optimizing the parameters of SAPF by Improved Particle Swarm Optimization (PSO) as well as Gravitational Search Algorithm (GSA).The results obtained are compared for conventional PI controller, PSO, GSA and PSOGSA. The results suggest the better performance of proposed work with PSOGSA based SAPF.

Keywords: Fuel Cell, Shunt Active Power Filter (SAPF), PSO, GSA, Power quality.

1. Introduction

In modern electrical power networks, the competition for green and clean energy is very much severe as compared to traditional energy sources because of environmental and social aspects. In addition to this the dependence on conventional energy resources is gradually decreasing due to their depleting nature and the emission of hazardous carbon and sulphur compounds. Thus, the generating companies are opting for generation of alternative energy from renewable sources, which are emission less, having better reliability and good power quality. But the integration of renewable energy with conventional power network is a tough challenge. One of the easier solutions to this challenge is use of micro grid. It is a concept applicable in places where the conventional power cannot reach. The solution for the energy crisis is the introduction of micro grid to the power system network with more utilization of nonconventional energy sources like solar power, wind power, fuel cell, geothermal energy etc. A micro grid basically comprises of several energy sources located randomly with less production rating and integrated to the

central grid with the help of specific converters as shown in the figure.1. The energy sources which are in remote locations can be functional independently without connecting to the grid in isolated mode or coupled to grid operation [1].

Hybrid electric power system based on a diesel generator is given in [2] connected to a Wind turbine, PV array and a lithium battery bank where the PV array MPPT utilizes the bipolar DC bus voltage equilibrium approach. Photovoltaic (PV) generation utilizes the direct conversion of solar irradiance into electrical energy. In modern scenario, it has proved to be an economic method for generating eco-friendly electricity with less environmental impact. In [3] the authors have emphasized on tracking the global maximum power point (GMPP) of PV array to counter the reduced yield of power due to partial shading conditions.

In another Endeavour a converter is developed by sharing the components between Cuk and SEPIC converters which works in both individual and simultaneous modes, based on the availability of source and prevents the need of input filter to eliminate the high frequency harmonics [4]. The efficiency of fuel cell which operates on proton exchange principle, known as PEMFC stack is evaluated in [5] and the corresponding results are utilized for forecasting of efficiency, output power and voltage rating and operational parameters of fuel cell stack. A numerical prototype for polymer electrolyte membrane (PEM) based fuel cells are evolved in [6] and logical explanations are obtained. It comprises of a gas diffuser, a catalyst layer, a cathode gas channel and a membrane. A hybrid source consisting of PEM fuel cell using hydrogen gas is given in [7] where water electrolyser system acts as a long-term storage and ultra-capacitor as short-term storage. The execution of PEM based fuel cell has been analysed analytically using pure hydrogen on the positive terminal and air on the negative terminal in [8] with distinct parameters.

Complex systems involving another type fuel cell known as, IRSOFC, was examined in [9] with an analytical prototype which describes consistency of fuel cell during simulation. This model has been studied with present test data. Transient flows, the reactant partial pressures, as well as loss mechanisms were studied with a dynamic fuel cell model where load transients were discussed in a fuel cell controlled by an inverter [10]. Energy management strategies with the aim of coordinated power flow to individual sources is given in [11] where optimization of energy flow is considered involving off-grid PV system, wind turbines and fuel cell. A multi-disciplinary hybrid system consisting of PV array, fuel cell and diesel generator to supply electric power to an off-grid system is discussed in [12], where load variation and solar energy variation are considered with the implementation of multi objective crow search algorithm (MOCSA). Real-time optimization (RTO) strategy [13] to obtain the optimal value of the fuel flow rate of a Hybrid Power System involving fuel cell for domestic purposes is discussed in [13] where the fuelling rate is limited by fuel cell current. Fuzzy logic controller is used to optimize the modified synchronous reference frame based SAPF in [14] where fuzzy controller is used to control the Capacitor voltage on DC side and a hysteresis controller is used to regulate the switching pulse fed to the inverter. In [15] the authors have discussed the operation of a fuel cell stack subjected to current harmonics where basic contribution of the inner double layered capacitor is explained.

The basic need for connecting a fuel cell stack or a PV array into a conventional grid demands the utilization of power electronic converters because the power produced in these energy resources are DC in nature. So, to synchronize them with ac micro grids, they must be converted to DC. For this purpose, many power electronic converters are available which transform the power from DC into AC domain. Introduction of these power electronic converters is the sole reason of induction of harmonics and transients in the power grid, which in turn reduce the quality of power. So, to boost the power quality issues, filtering of energy is very important. For this errand passive filters like inductors, capacitors or their combination can be used in passive power filtering. But these elements can only perform in static conditions. To enhance the attributes of electricity dynamically the need of active power filtering is obvious.

The use of classical and predictive direct power control for shunt active power filter is proposed in [16] for reduction of current harmonics. Magnitude of the basic component of current in the series filter is regulated by an error signal generated by comparing the load voltage with a pre-defined reference, which permits an appropriate modification of power factor, THD and modulation of voltage at load level [17].

A five-level inverter-based shunt active power filter (SAPF) connected to a photovoltaic system is proposed in [18] where active-reactive power approach is introduced for the SAPF. The DC bus voltage control technique by using three reference currents for three phase SAPF is discussed in [19] for balanced and unbalanced load conditions where goal is to reduce the THD, lower the amplitude of neutral current and eradicate the neutral currents caused by fluctuating nonlinear loads.

Further to improve the performance, the SAPF and PI controller parameters are optimized and simulated which produce different results. The PI controller based SAPF is tuned using three swarm-based optimization techniques such as PSO, Bacteria foraging for elimination of harmonics in [20-21]. The UPFC based controller is used and PSO helps to tune the Eigen values with multi objective function consisting of damping factor of the un-damped electromechanical modes. PSO based fuzzy controller is proposed in [22-23] in a load frequency model. Adaptive-Neuro-Fuzzy Inference System (ANFIS) based MPPT is proposed in [24] for increasing the performance of the PV panel for varying atmospheric conditions. In [25] GSA is used for concurrent coordinated construction of the PSS and TCSC for power system damping. In reference [26] the energy and operation management of renewable micro grids is discussed under uncertain environment with the help of self-adaptive GSA.

The solar power generation has certain draw backs like intermittent and nonlinear in nature, depends on environmental conditions like temperature, humidity etc. The power generation is non-uniform throughout the year, that is in rainy season irradiance emission reduces which leads the interruption of power followed by partial shading effect. The design of PV panel includes PV array, MPPT controller, converters and inverters. The power electronic devices are highly complex and acts as source of harmonics for which additional equipment like filters are required to be installed. Thus, other alternative renewable sources like fuel cell is considered for this paper.

In this working model a fuel cell coupled micro grid is designed with SAPF. Different power quality issues like voltage sag, swell, transient and harmonics are simulated in different loading condition. To enhance the filter capacity, PSO, GSA and PSOGSA are applied, to find optimized values of the design parameters. The results of different methods are compared.

The rest part of the work is placed in this paper as per the following manner. In section 2 the model under study is described. The methods for optimization used in this work are discussed in section 3. Simulation results for both rectifier as well as dynamic load are placed in section-4. Section-5 deals with the motivations and contributions. The conclusion and future scope for this model is discussed in section-6.

2. Micro grid structure

The figure shown below is a complete model representation of a micro grid. Different local generations like, solar, wind, fuel cell, diesel generator, small hydro plants etc. are collectively used as sources of the micro grid. The basic block diagram of a micro grid is given in Fig. 1.

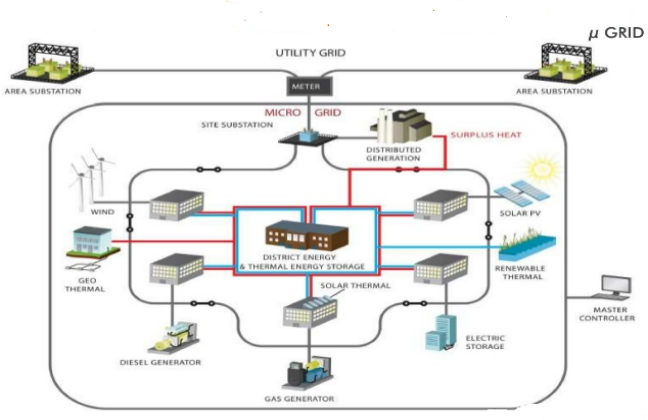

Figure.1: General structure of micro grid.

In this paper a small part of the entire micro grid is studied and the harmonics reduction is investigated as given in the Fig. 2. The discussed model where a fuel cell stack is connected to a DC capacitor followed by a three-phase bridge converter and integrated with a grid. At PCC a SAPF is attached to the model through a three-phase breaker. A shunt active power filter is placed at PCC followed by the output of the bridge converter. The model is simulated with a nonlinear rectifier load and the results are depicted.

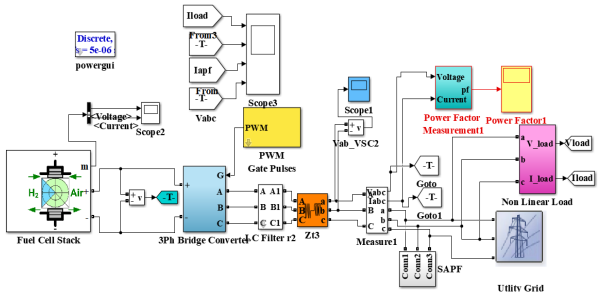

Figure.2: Simulation diagram of the micro grid model

2.1 Inverter:

The three-phase bridge inverter is used to convert the DC Voltage generated in the fuel cell stack to AC waveforms. Basically a 3 leg MOSFET is used as a bridge inverter. A Pulse Width Modulator is being used to generate the pulse at the gate terminal of the Bridge converter.

2.2 *Fuel Cell:*

The structure and function of a Fuel cell is almost same as a battery, which has two electrodes and an electrolyzing agent which produces electricity. Nevertheless, there is a remarkable difference between fuel cell and battery. The fuel cell produces energy from external source whereas battery from its own electrolyte.

The second difference is the electrolyte in the fuel cell is sandwiched and the electrodes exchange electrons through this medium and in the battery the liquid electrolyte carries the ions. Constant utilization of fuel causes emission by-products continuously in a fuel cell. This emitted by-product is very less dangerous and more eco-friendlier as compared to other traditional energy sources. Also, the fuel cell heat is generated as a by-product and can be used in different applications. The fuel cell is superior and more efficient than steam turbine generator, since there are no movable parts and chemical energy is directly converted to electrical energy. In some applications a fuel stack is designed with combination of many fuel cells with anode, cathode and electrolyte layer. The electro chemical equations inside a SOFC when hydrogen is used as fuel are given by

$$H_2 + o^{2-} \rightarrow H_2o + 2e^- \quad (1)$$

$$\frac{1}{2}o_2 + 2e^- = o^{2-} \quad (2)$$

$$\frac{1}{2}o_2 + H_2 = H_2o \quad (3)$$

In case of carbon monoxide fuel is used in SOFC the electrochemical reactions are,

$$2Co + 2O^{2-} \rightarrow 2Co_2 + 4e^- \text{ At anode.} \quad (4)$$

$$O_2 + 4e^- \rightarrow 2O^{2-} \text{ At cathode.} \quad (5)$$

General cell reaction is presented as

$$2Co + o_2 \rightarrow 2Co_2 \quad (6)$$

At high temperature Co can be converted to Co_2 and hydrogen gas as the water –gas reaction.

$$2Co + 2H_2o \rightarrow 2Co_2 + 2H_2$$
$$2H_2 + 2o^{2-} \rightarrow 2H_2o + 4e^- \quad (7)$$

2.2.1. Electro chemical Model:

The net output voltage of SOFC is reduced from its open circuit voltage due to some permanent losses. Several phenomena give to irreparable drop in genuine output voltage. The vital losses are due to over voltage and polarization in fuel cell.

The real cell voltage $V_{ac} < E$ and is calculated by

$$V_{Oac} = E - losses = E\eta_{total} \quad (8)$$

Where η_{total} is the total ohmic loss

2.3 Non-linear load:

A nonlinear load is connected to the model, which consists of a three-phase rectifier load. The rectifier load is the combination of a resistive load of 10 ohms and an inductive load of 10mili Hennery connected in series. The rectifier load is connected to the grid with the help of a three-phase breaker. The three-phase breaker provides the option of connecting the load or cutting the load at any time of operation.

2.4 Shunt Active Power Filter (SAPF):

The SAPF works on injection of a compensating current in opposition to harmonics currents. The SAPF injects the same current at PCC through an inverter. Another important purpose is to make the source current free of fluctuation and to align it in phase with source voltage disregarding the load characteristics. Fig. 3 shows the basic reimbursing phenomenon of SAPF. Fig. 4 denotes the control structure and working of a SAPF while Fig. 5 gives the basic idea about circuit of SAPF.

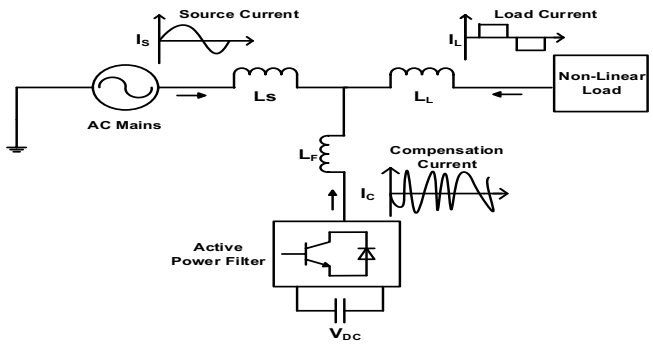

Figure.3: Shunt active power filter

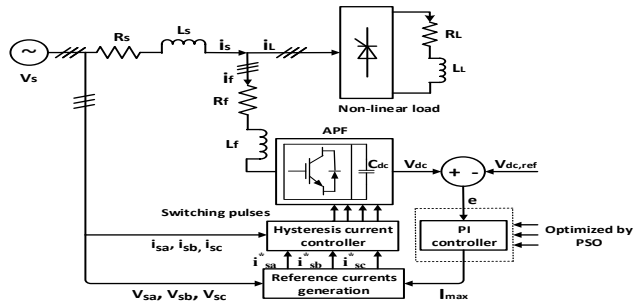

Figure.4: Control structure of SAPF

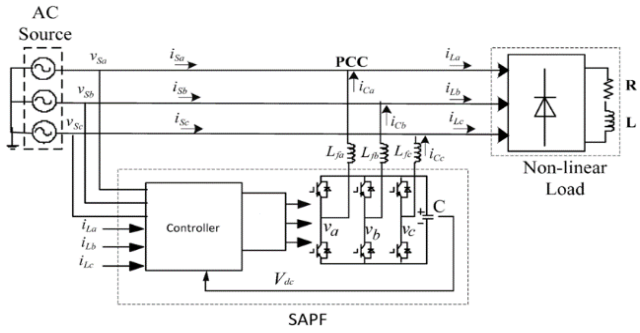

Figure.5: circuit diagram of SAPF.

2.5. Generation of supplied source current:

The fundamental compensating principle of a SAPF is to extract or contribute a compensating current i_c from or to the transmission line, as a result of which source current and the source voltage align in same phase by mitigating the current harmonics. The source current is given by:

$$i_{source}(t) = i_{load}(t) + i_{comp}(t) \quad (9)$$

Similarly, instantaneous source voltage can be represented mathematically as:

$$v_s(t) = v_m \sin \omega t \quad (10)$$

The fundamental and harmonic components of current can be given by

$$i_l(t) = \sum_{n=1}^{\infty} i_n \sin(2\pi fnt + \theta_n) = i_1 \sin(2\pi ft + \theta_1) + \sum_{n=2}^{\infty} i_n \sin(2\pi fnt + \theta_n) \quad (11)$$

The momentary power across the load is represented as:

$$\begin{aligned} p_{load}(t) &= v_{source}(t) * i_{load}(t) = v_m I_{load} \sin^2 2\pi ft * \cos\theta_1 + \\ & v_m I_1 \sin \pi ft * \cos 2\pi ft * \sin\theta_1 \\ & + V_m \sin 2\pi ft * \sum_{n=2}^{\infty} i_n \sin(2\pi fnt + \theta_n) \\ &= p_f(t) + p_r(t) + p_n \end{aligned} \tag{12}$$

From equation (12), active power drawn by the load is

$$p_f(t) = V_m I_1 \sin^2 2\pi ft * \cos\theta_1 = v_s(t) * i_s \tag{13}$$

From equation (13) the reimbursing current generated during compensation is:

$$i_s(t) = \frac{p_f(t)}{v_s(t)} = I_1 \cos\theta_1 \sin 2\pi ft = I_{sm} \sin 2\pi ft \tag{14}$$

Where $I_{sm} = I_1 \cos\phi_1$ (15)

In addition, the PWM converter is associated with loses due to switching. For this reason, in return the system should provide a little swell owing to the losses due to capacitor leakage and converter switching with the active power drawn by the load. For this reason, the maximum source current is expressed as

$$i_{spl} = i_{sm} + i_{sl} \tag{16}$$

In (16) i_{sl} denotes maximum value of the loss current i_s which must be aligned along (in phase) the service voltage and properly sinusoidal, if the proposed filter generates the reactive power with harmonics. Hence, the SAPF should generate the compensating current as given below:

$$i_c(t) = i_L(t) - i_s \tag{17}$$

Hence, for measuring instantaneous value of compensation current due to the reactive power with harmonics, it is essential to determine i_s.

3. Optimization techniques

In designing of shunt active power filter with SOFC based micro grid, many parameters are selected randomly, which affects the performance. Setting the optimum values of the parameters is a tough challenge. Thus, various optimization techniques like PSO, gravitational search algorithm are applied and further to improve the strength of the algorithms, hybridization of PSO and GSA is formulated and applied for the same purpose. Hence in this model the above optimization methods are utilized to optimize the values of the design variables. Six parameters are being optimized such as $k_p, k_i, L_f, R_f, C_{dc}$ and v_{deref}. PSO, GSA and their hybridization PSOGSA are used to optimize the six variables as given above.

3.1 Particle Swarm Optimization Algorithm PSO:

The idea of PSO operation basically based on techniques of bird flocking. In this algorithm a large number of particles are used as aspirant solution randomly moving in the search area to obtain an overall best solution. The location of every element is expelled by its best position, P_{best} and g_{best}. In each step every individual particle updates its velocity and position by the use of following equations.

$$vl_i(n+1) = \omega \times vl_i(n) + c_1 \times n_{rand} \times \{P_{best} - x_i(n)\} \tag{18}$$

$$x_i(n+1) = x_i(n) + vl_i(n+1) \tag{19}$$

Here $vl_i(n)$ is the speed of i_{th} particle in the iteration n and w is the weight and n_{rand} is the arbitrary number selected in the range of [0, 1]. $x_i(n)$ The position of i_{th} particle in n_{th} iteration, c_1, c_2 are two positive constants selected arbitrarily and controls the weighting factors accountable for changing the speed of every element towards P_{best} and g_{best}. Equation (19) represents the position up gradation in each step. Analysis of velocity equation says that the first term $\omega \times V_i(n)$ gives information about PSO investigation capability and the second term $c_1 \times n_{rand} \times \{P_{best} - x_i(n)\}$ represents personal thoughts and co action of particles. In each iteration the speed is calculated and that is used for position modification. The process will continue till the stopping criterion is researched.

3.2 Gravitational Search Algorithm (GSA):

GSA is an evolutionary algorithm following Newton's law of gravitation. This technique relates mass and gravity interactions. In the nature inspired GSA method, the agents inside search space are attached with each other by gravitational force. The movement of each element is dependent upon its mass. Each agent travels towards agents of higher mass. The mathematical expressions of the GSA are given below.

Definition 1. The inertial mass represents fitness of the particle, which is calculated as following.

$$\begin{cases} m_i(t) = \dfrac{fit_i(t) - worst(t)}{best(t) - worst(t)} \\ M_i(t) = \dfrac{m_i(t)}{\sum_{j=1}^{N} m_j(t)} \end{cases} \tag{20}$$

Where $fit_i(t) =$ fitness of the particles.

$best(t) =$ Optimal result at time t.

$worst(t) =$ Most horrible resolution at time t.

$M_i(t) =$ Mass of particle x_i at time t.

Definition 2. The gravitational force between i_{th} and j_{th} particle in k dimension is given by

$$F_{ij}^{k}(t) = G(t)\frac{M_{bj}(t)\times M_{aj}(t)}{R_{ij}(t)+\varepsilon}\left(x_j^k(t)-x_i^k(t)\right) \tag{21}$$

Where ε is constant and M_{aj}, M_{bi} are the mass of object j and i respectively. The universal gravitational constant is given by

$$G(t) = G_0 \times e^{-\frac{\alpha}{T}} \tag{22}$$

G_0= the value of gravitational constant initially, and set to 100. $\alpha = 20$, T is ultimate iteration count and $R_{ij}(t)$ is the space among the particles i and j.

Definition-3: the acceleration due to gravity between the particles i and j is calculated by the following

$$a_i^k(t) = \frac{F_i^k(t)}{M_i(t)} \tag{23}$$

Here $M_i(t)$ is mass.

Using the following formula, the speed and location of the individual i is simplified according to the acceleration.

$$\begin{aligned} vl_i^k(t+1) &= rand_i \times vl_i^k(t) + a_i^k(t) \\ x_i^k(t+1) &= x_i^k(t) + vl_i^k(t+1) \end{aligned} \tag{24}$$

3.2.1. Pseudo Code of Gravitational search Algorithm.

1. Initialization: let t=1 and select a random set of feasible solution and a set of velocities.

$$x^t = \{x_1^t, x_2^t \ldots\ldots\ldots x_N^t\}, \quad v^t = \{v_1^t, v_2^t \ldots\ldots\ldots v_N^t\}$$

2. While stopping criterion is not satisfied do.
3. Fitness evaluation: The objective function $f(x_i^t)$ is evaluated for each resolution (mass) in the present population x^t.
4. $G^t or G_{chaotic}^t$, $best^t$, $worst^t$ and M_i^t are updated using the above equations.
5. Computation of total force: Compute F_{ij}^k and F_i^k.
6. Update: Compute a_i^t, v_i^{t+1} and x_i^{t+1}
7. End while

3.3 PSOGSA Optimization:

To overcome the draw backs of both algorithms PSO and GSA are hybridized to form a new inhabitant based evolutionary technique referred as PSOGSA. Major benefit of PSOGSA is to amalgamate the efficient management in PSO and investigation ability of GSA. The speed and location are modified as

$$\begin{aligned} u_i(n+1) &= \omega \times u_i(n) + c_1' \times n_{rand} \times ac_i(n) + \\ & c_2' \times n_{rand}\{g_{best} - x_i(n)\} \end{aligned} \tag{25}$$

$$x_{pi}(n+1) = x_{pi}(n) + u_i(n+1) \tag{26}$$

Here $u_i(n)$ is speed of i_{th} element. ω is the weight factor and c_1, c_2 are the coefficients of acceleration. In this model, in PSOGSA optimization the aspirant outcomes are presuming the representative of an arbitrarily created inhabitant. First the population is initialized with GSA, the constant G is computed then robustness value of explored elements is estimated along with mass and acceleration. The above equations represent velocity and position of PSO-GSA. The best solutions are modified in each iteration. The above process is repetitive until the projected system reaches termination criterion. The same is presented as following. Fig. 6 represents the basic flow chart of proposed PSOGSA optimization algorithm.

Objective Function:

The proposed design problem can be framed as the following optimization problem.

The cost function (β) is minimized subject to

$$Z_{\min} < Z < Z_{\max}$$

Where Z is the vector which consists of the SAPF controller parameters.

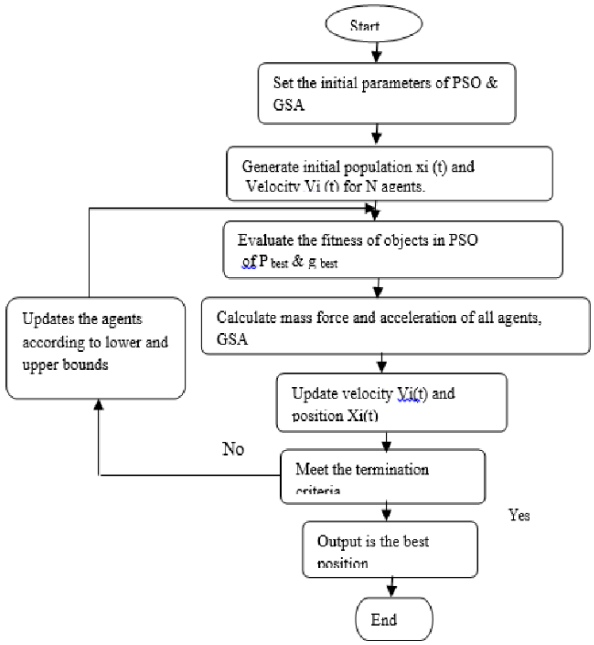

Figure.6: flow chart of PSOGSA

4. Results and discussions

4.1. Islanding Mode of operation

In this case, the PSO-GSA algorithm is applied to investigate the power quality issues of a fuel cell based micro grid without grid connection. The inverter of DG works on PWM controller operating mode. The SOFC voltage increases from zero to 300 volt. The real and reactive power has been improved as depicted by the following figures. The islanding operation the most formidable mode for the study of power quality issues. For effective performance of the "PSOGSA" for compensating of voltage disturbances, the output filter of the inverters has been designed as LC-filters. Fig. 7 represents the voltage and current waveforms of the fuel cell in islanded mode of operation. Fig. 8 shows the real and reactive power variations during islanding mode for both conventional PI controller as well as PSOGSA optimized PI controller. In both cases the minimization of power fluctuation can be observed with modern PSOGSA technique.

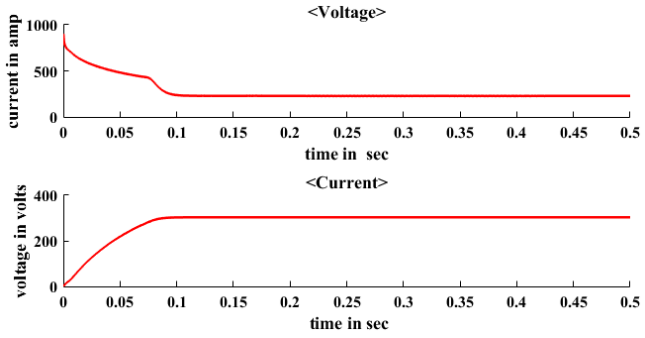

Figure.7: Voltage and current in islanding mode

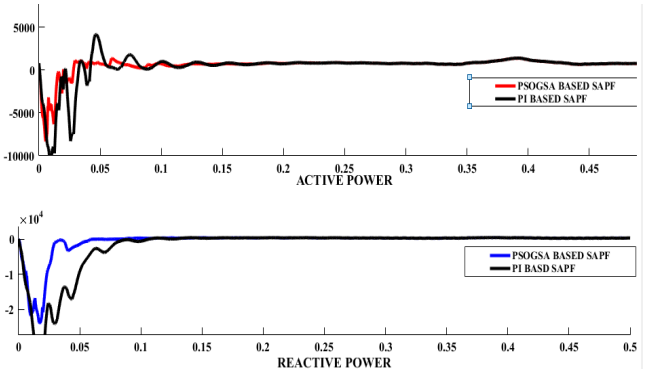

Figure.8: Active and reactive power in islanding mode.

4.2. On Grid Mode of Operation:

In his case study the model is integrated with a grid and simulated with nonlinear loads like three phase rectifier load and dynamic load. The results are depicted from the following figures.

4.2.1. Three phase rectifier load:

The three-phase rectifier load consists of a resistor having resistance of 10 ohms and an inductor having inductance of 40 mH is connected in series, which are connected to a bus through six diodes. Out of the six diodes only two diodes are active anytime for supplying load current for a single phase and hence for three phase's six diodes operate at random.

The six design variables are optimized using conventional PI controller, PSO, GSA and PSOGSA. The results obtained are compared for THD in four cases. The optimized values of the six discussed variables are provided in table-1. The THD values for the load current are compared and given in Table 2. The values for the source current THD are calculated and given in Table 3. and Table 3 also contain the source side power factor for all the three phases for simulation through different optimization processes.

Fig. 9 represents the grid active power curve where the red line denotes the active power variation through SAPF optimized with PSOGSA. The black line denotes the active power at grid where SAPF is utilized with conventional PI controller.

Fig. 10 shows the reactive power variation at the grid, where the red curve denotes least variation in reactive power flow due to optimized SAPF with PSOGSA as compared to the black line with SAPF with Conventional PI controller and black line without SAPF.

Fig. 11 represents the Fuel cell voltage. From this figure it can be clearly verified that the blue line where PI controller is connected shows more fluctuation in voltage as compared to the red line where PSOGSA based SAPF is utilized.

The grid voltage with Optimized SAPF is shown in Fig. 12. Fig. 13 represents the grid voltage with PI based SAPF. In Fig. 14 the grid voltage is given where a three-phase fault is being connected to the line for 0.1 t0 0.2 second. From these figures it can be clearly observed that without SAPF there is a voltage sag from 0.1 to 0.2 second as shown in Fig. 14. The application of PI based SAPF can improves the voltage sag but still there are some transients as denoted in Fig. 13. Finally, with the application of PSOGSA based SAPF the waveform can be made sinusoidal as given in Fig. 12.

Fig. 15 and Fig. 16 represents the harmonic analysis of load current and source current respectively for SAPF based on conventional PI controller where the THD of the load current is 13.47% in one of the phases and source current THD is found to be 10.66%. This shows the higher value of THD in both waveforms.

Fig. 17 and Fig. 18 denotes the FFT analysis of load and source currents for PSO based SAPF. In the technique THD of the load side current is minimized to 7.37% and THD of source is decreased to 6.37%. Hence PSO based SAPF is more useful in minimizing harmonics over Conventional PI controller based SAPF.

Fig. 19 and Fig. 20 shows the harmonic distortion measurement of load current and source current through GSA based SAPF. Through GSA the load current THD is minimized to 5.53% and the source current THD is minimized to 3.39%, which shows the superiority of GSA over PSO based SAPF.

Fig. 21 and Fig. 22 denotes the harmonic distortion of load current and source current of PSOGSA based SAPF. With the help of hybrid PSOGSA technique the load current harmonic is reduced to 2.41% and source current THD is limited to 1.49%.

The results prove the improvisation of THD in PSOGSA based SAPF as compared to GSA, PSO and PI based SAPF. Eq. 27 represents the relationship between Power factor and THD.

$$PF = \cos\theta * \left(\frac{1}{\sqrt[2]{(1+THD^2}} \right) \quad (27)$$

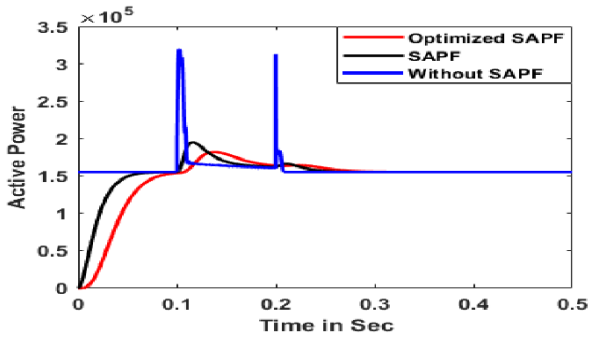

Figure.9: Grid active power

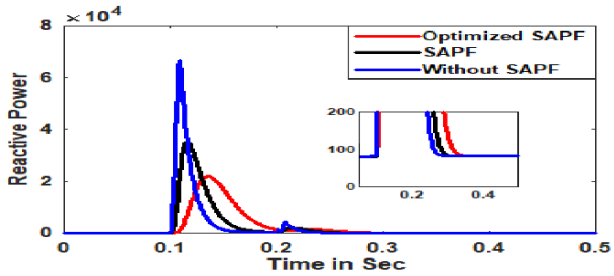

Figure.10: Grid reactive power

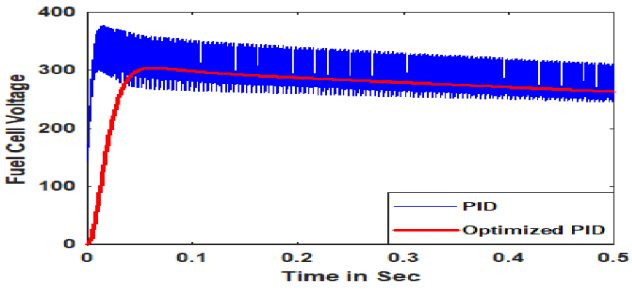

Figure.11: SOFC voltage

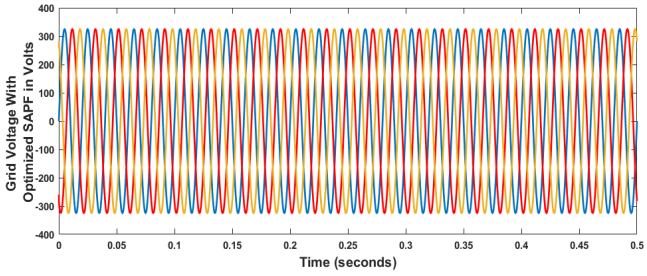

Figure.12: Grid voltage with optimized SAPF

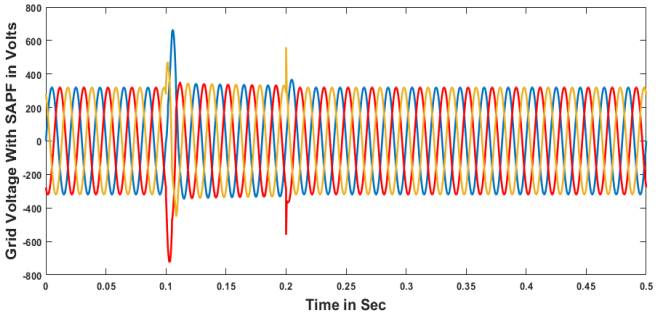

Figure.13: Grid voltage with PI based SAPF

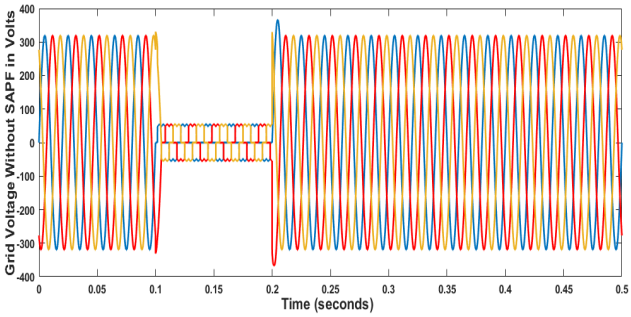

Figure.14: Grid voltage with PI and without SAPF

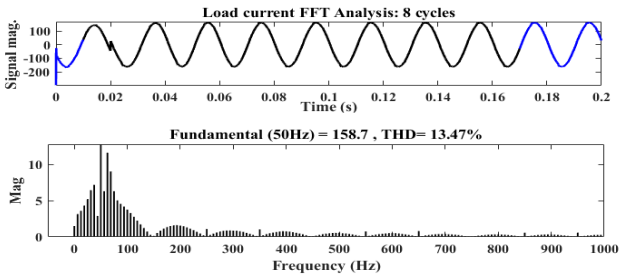

Figure.15: FFT analysis of load current with PI -SAPF

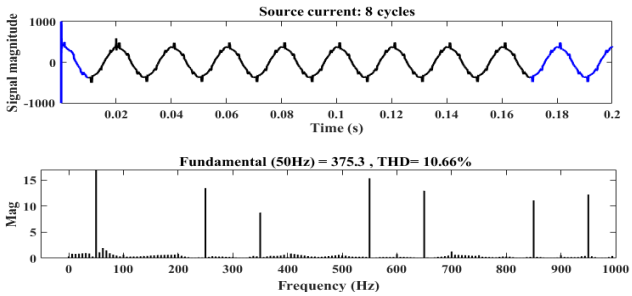

Figure.16: FFT analysis of source current with PI SAPF

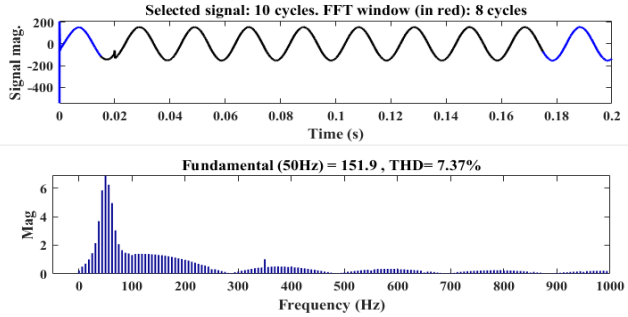

Figure.17: FFT analysis of load current PSO-SAPF

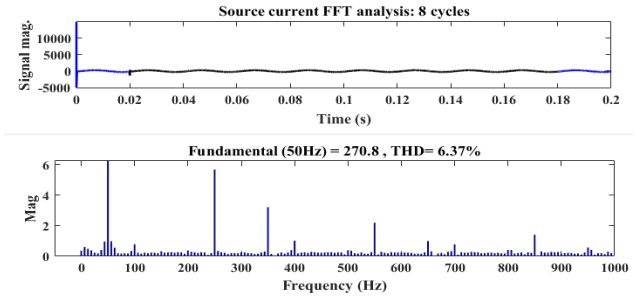

Figure.18: FFT analysis of source current with PSO-SAPF

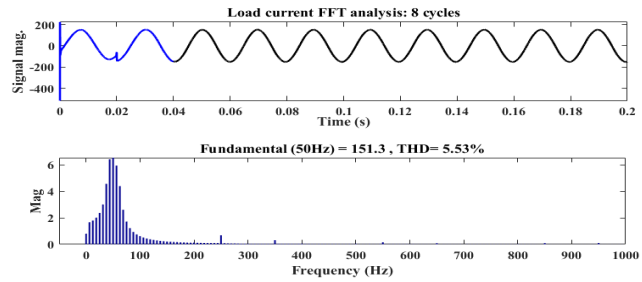

Figure.19: FFT analysis of load current with GSA-SAPF

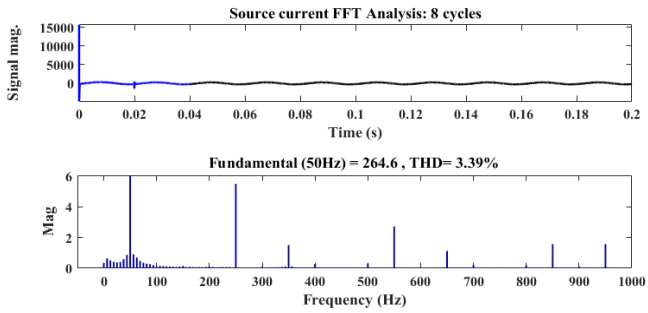

Figure.20: FFT analysis of source current with GSA based SAPF

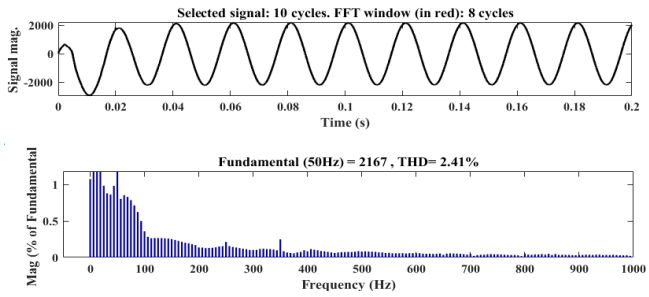

Figure.21: FFT analysis of load current with PSOGSA-SAPF

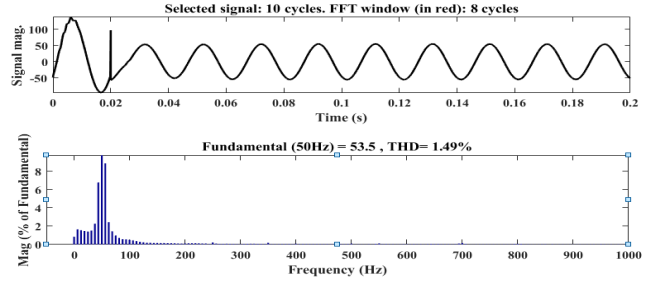

Figure.22: FFT analysis of source current with PSOGSA-SAPF

Table-1: Parameters Obtained After Optimization

	k_p	k_i	c_{dc} (μF)	v_{dcref} $(volt)$	L_f (mH)	R_f (Ω)
PI	0.57	10.3	2000	3200	0.57	1
PSO	0.025	39.98	3000	3000	0.660	0.227
GSA	0.988	12.57	3400	3317	0.343	0.099
PSO GSA	0.432	2.832	3100	3672	0.231	0.085

Table-2: Load current FFT analysis

	%THD		
phases	a	b	c
	11.30	13.47	10.67
PSO	7.37	9.84	8.75
GSA	5.53	6.58	6.54
PSOGSA	2.41	2.49	2.72

Table-3: Source current FFT analysis

	%THD			Source Power Factor		
Phases	a	b	c	a	b	c
PI	10.66	11.27	11.28	0.9903	0.9897	0.9903
PSO	6.37	6.46	7.24	0.9910	0.9908	0.9909
GSA	5.53	6.58	6.54	0.9956	0.9957	0.9984
PSO GSA	1.49	1.74	2.11	0.9998	0.9997	0.9999

4.2.2. Dynamic load:

A three-phase dynamic load is connected as the load to the bridge converter output through an LC filter. The dynamic load is a three phase three wire system where the active power and reactive power fluctuate as a function of the positive sequence component of voltage and hence negative and zero sequence components are nullified. Fig. 23 represents the three-phase waveform of load current, SAPF current, source current and source voltage of a PSOGSA optimized SAPF, where a dynamic load is connected to the fuel cell grid connected model.

Fig. 24 and Fig. 25 denote the load & source current FFT analysis of a PI - SAPF where the THD is as high as 13.45

in one of the load current phases and up to 10.38 in source current phases.

Fig. 26 and Fig. 27 represent the PSO based SAPF, where the load current THD is minimized to 9.81 and source current THD is lowered to 8.80%.

GSA based SAPF is utilized and the resultant curves are given in Fig. 28 and Fig. 29. It can be seen that the harmonic distortion is further reduced to 7.17 in load current and 5.82 in source current.

The hybrid PSOGSA optimization technique is applied to the SAPF and it can be found that the load current THD is reduced to 2.39% and source current THD is limited to 2.35%. Fig. 30 and Fig. 31 represent these curves.

Table 4 denotes the THD level of all the three phases in load current for all the discussed optimization techniques whereas Table 5 demarcates the harmonic variation of source current in all the three phases for given optimization techniques. Table 3 and Table 5 also show the source side power factor for all the cases and techniques. The comparison of results shows that PSOGSA can be useful in limiting the harmonics in load side current and source side current more effectively. Also, tabulation confirms that power factor of the source side is closer to unity in PSOGSA optimization technique.

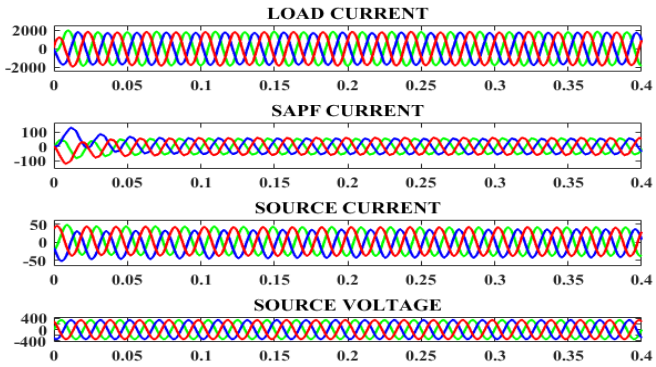

Figure.23: Three phase waveform (I_{LOAD}, I_{SAPF}, I_{SOURCE}, V_{SOURCE}) with PSOGSA based SAPF

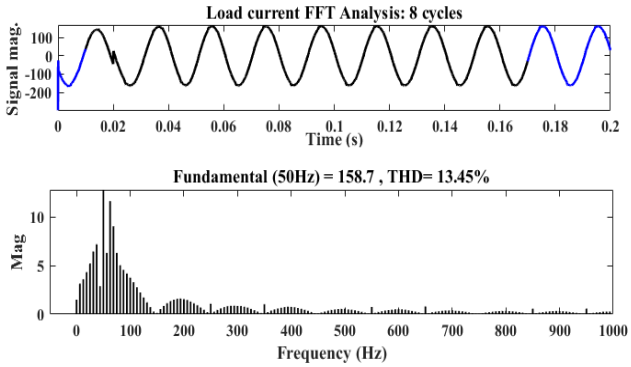

Figure.24: FFT analysis of load current with PI -SAPF

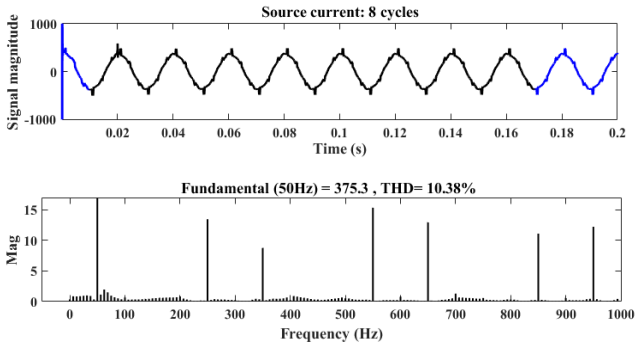

Figure.25: FFT analysis of source current with PI-SAPF

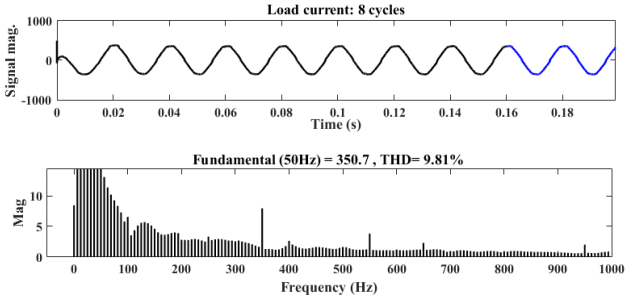

Figure.26: FFT analysis of load current with PSO - SAPF

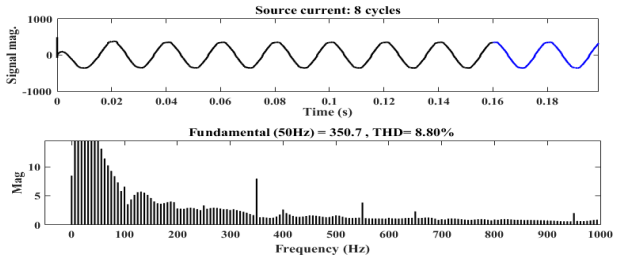

Figure.27: FFT analysis of source current with PSO based SAPF

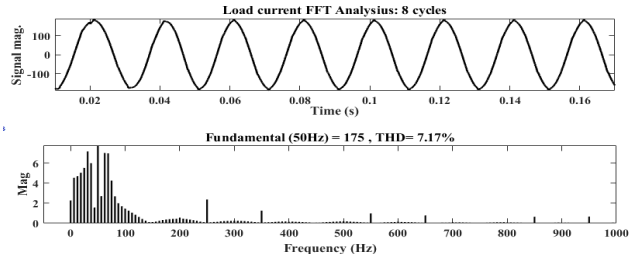

Figure.28: FFT analysis of load current with GSA based SAPF

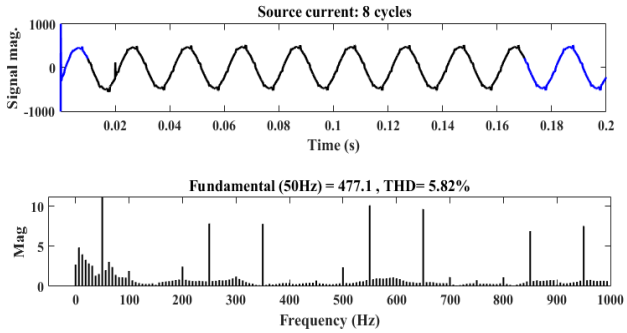

Figure.29: FFT analysis of source current with GSA based SAPF

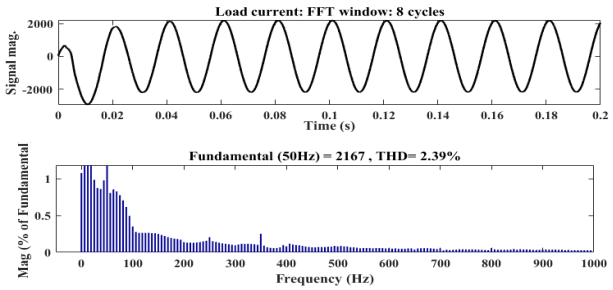

Figure.30: FFT of load current with PSOGSA - SAPF

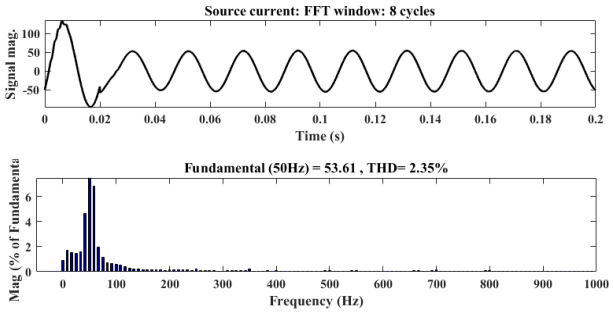

Figure.31: FFT of source current with PSOGSA-SAPF

Table-4: Load current FFT analysis

	%THD		
Phases	a	b	C
PI	12.37	13.45	11.87
PSO	8.31	9.81	8.75
GSA	7.17	6.58	6.92
PSOGSA	2.38	2.39	2.72

Table-5: Source current FFT analysis

	%THD			Source Power Factor		
Phases	a	b	c	a	B	c
PI	10.38	10.87	10.28	0.9917	0.9853	0.9911
PSO	8.97	8.80	8.24	0.9927	0.9931	0.9924
GSA	5.85	5.98	5.82	0.9976	0.9963	0.9989
PSOGSA	2.49	2.74	2.35	0.9993	0.9998	0.9999

The convergence characteristics for various optimization techniques discussed in this paper are shown in figure-32. The PSO optimization has taken nearly 135 iterations to converge, GSA has taken 32 iteration for convergence while the hybrid PSOGSA technique has spent only 24 iterations for convergence. This shows the quick converging behaviour of proposed PSOGSA method.

1. Motivation and contribution

In the discussed literature many papers have given the working and implementation of different fuel cell models either connected to grid or standalone. The working of SAPF along with different techniques such as SRF and MSRF are also mentioned, but the parametric optimization of SAPF is not mentioned anywhere with fuel cell. In this paper six parameters of SAPF were optimized with the new hybrid PSOGSA algorithm aiming for minimization of THD in load and source current. The improvement in power quality is shown in the tabulation.

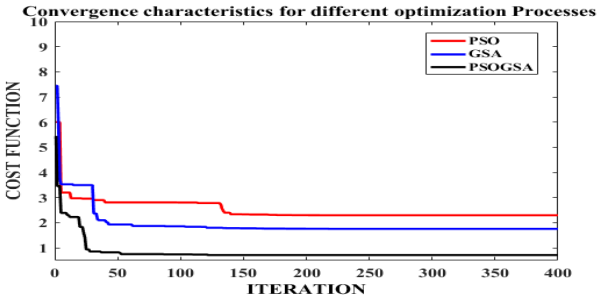

Figure.32: Convergence characteristics for different optimization techniques

2. Conclusion

The proposed model is successfully simulated in MATLAB/Simulink environment where a fuel cell stack is integrated to the grid with the help of a three-phase boost converter. The model with SAPF is simulated for four different methods like PI-SAPF, PSO-SAPF, GSA-SAPF and PSO-GSA-SAPF in two different operating conditions. The FFT analysis and real and reactive power simulation with a fault is depicted in the above figures. The fuel cell model with SAPF is simulated for both loading conditions such as three phase rectifier load and a three-phase dynamic load. The tabulation proves the superiority of PSO-GSA-SAPF over GSA, PSO and conventional PI-controller and is able to achieve the IEEE standard (Within 5%) of THD.

Re f e r e n c e s:

[1] Katiraei, Faridaddin, Mohammad Reza Iravani, and Peter W. Lehn, “Micro-grid autonomous operation during and subsequent to islanding process”, IEEE Transactions on power delivery, Vol. 20, No.1, pp. 248-257, 2005, (Article).

[2] M. M. G. Lawan , J. Raharijaona , M.B. Camara , B. Dakyo , “Power control for decentralized energy production system based on the renewable energies—using battery to compensate the wind/load/PV power fluctuations”, 6th International Conference on Renewable Energy Research and Applications (ICRERA), pp. 1132-1138, IEEE, 2017, (Conference Paper).

[3] K. Chen, S. Tian, Y Cheng, L. Bai, “An improved MPPT controller for photovoltaic system under partial shading condition." IEEE transactions on sustainable energy, Vol.5, No. 3, pp. 978-985. (2014), (Article).

[4] S. Choudhury, P.K. Rout, "Design of fuzzy and HBCC based adaptive PI control strategy of an islanded microgrid system with solid-oxide fuel cell", International Journal of Renewable Energy Research (IJRER), Vol.7, No. 1, pp. 34-48, 2017, (Article).

[5] J.M. Corrêa, F.A. Farret, L.N. Canha, "An electrochemical-based fuel-cell model suitable for electrical engineering automation approach" ,IEEE Transactions on industrial electronics , Vol.51, No. 5, pp.1103-1112, 2004, (Article).

[6] V. Gurau, F. Barbir, H. Liu, "An analytical solution of a half-cell Model for PEM fuel cells", Journal of the Electrochemical Society, Vol. 147, No. 7, pp.2468-2477, 2000, (Article).

[7] B. Zafar, "Design of a Renewable hybrid photovoltaic-Electrolyze-PEM/Fuel Cell System using Hydrogen Gas", International Journal of Smart Grid-ijSmartGrid, Vol. 3, No. 4, pp.201-207, 2019, (Article).

[8] L. Wang, A. Husar, T. Zhou, H. Liu, "A parametric study of PEM fuel cell performances." International journal of hydrogen energy, Vol. 28, No. 11, pp. 1263-1272, 2003, (Article).

[9] A.F. Massardo, F. Lubelli, "Internal reforming solid oxide fuel cell-gas turbine combined cycles (IRSOFC-GT): Part A-Cell model and cycle thermodynamic analysis", J. Eng. Gas Turbines Power, Vol. 122, No. 1, pp.27-35, 2000, (Article).

[10] P. Famouri, R.S. Gemmen, "Electrochemical circuit model of a PEM fuel cell." In 2003 IEEE Power Engineering Society General Meeting (IEEE Cat. No. 03CH37491), Vol. 3, pp. 1436-1440. IEEE, 2003, (Article).

[11] A.L. Bukar, C.W. Tan, "A review on stand-alone photovoltaic-wind energy system with fuel cell: System optimization and energy management strategy." Journal of cleaner production, Vol. 221, pp.73-88, 2019, (Article).

[12] M. Jamshidi, A. Askarzadeh, "Techno-economic analysis and size optimization of an off-grid hybrid photovoltaic, fuel cell and diesel generator system", Sustainable Cities and Society, Vol. 44, pp. 310-320, 2019, (Article).

[13] N. Bizon, A.G. Mazare, L.M. Ionescu, F.M. Enescu, "Optimization of the proton exchange membrane fuel cell hybrid power system for residential buildings", Energy Conversion and Management, Vol.163, pp. 22-37, 2018, (Article).

[14] P.K. Barik, G. Shankar, P.K. Sahoo, "Power quality assessment of microgrid using fuzzy controller aided modified SRF based designed SAPF", International Transactions on Electrical Energy Systems, Vol. 30, No. 4, 2020, (Article).

[15] G. Fontes, C. Turpin, S. Astier, "Interactions between fuel cells and power converters: Influence of current harmonics on a fuel cell stack", IEEE Transactions on Power Electronics, Vol. 22, No. 2 pp.670-67, 2007, (Article).

[16] O. Aissa, S. Moulahoum, I. Colak, "Analysis, design and real-time implementation of shunt active power filter for power quality improvement based on predictive direct power control", IEEE International Conference on Renewable Energy Research and Applications (ICRERA), pp. 79-84,2016, (Conference Paper).

[17] J.W. Dixon, G. Venegas, L.A. Moran, "A series active power filter based on a sinusoidal current-controlled voltage-source inverter", IEEE, Industrial Electronics, Vol.44, No. 5, pp. 612-620, 1997, (Article).

[18] Y. Abdelkader, T. Allaoui, C. Abdelkader, "Power Quality Improvement Based on Five-Level Shunt APF Using Sliding Mode Control Scheme Connected to a Photovoltaic", International Journal of Smart Grid-ijSmartGrid, Vol. 1, No. 1 ,pp. 9-15, 2017, (Article).

[19] A. Chebabhi, M.K. Fellah, A. Kessal, M.F. Benkhoris, "Comparative study of reference currents and DC bus voltage control for Three-Phase Four-Wire Four-Leg SAPF to compensate harmonics and reactive power with 3D SVM", ISA transactions, Vol. 57 ,pp.360-372, 2015, (Article).

[20] R. Singh, A.K. Singh, P. Kumar, "Comparison of three evolutionary algorithms for harmonic mitigation using SAPF", 6th International Conference on Industrial and Information Systems. IEEE, pp. 392-397, 2011, (Conference Paper).

[21] H. Shayeghi, H.A. Shayanfar, S. Jalilzadeh, "A PSO based unified power flow controller for damping of power system oscillations", Energy conversion and management, Vol. 50, No. 10, pp. 2583-2592, 2009, (Article).

[22] E. Assareh, M. Biglari, "A novel approach to capture the maximum power from variable speed wind turbines using PI controller, RBF neural network and GSA evolutionary algorithm", Renewable and Sustainable Energy Reviews, Elsevier, Vol. 51, pp. 1023-1037, 2015, (Article).

[23] D. P. Acharya, N. Nayak, S. Choudhury, "Power Quality Enhancement of a Photovoltaic Based Micro Grid System Using Optimized Fuzzy Controller with SAPF", International Conference on Smart Systems and Inventive Technology (ICSSIT), pp. 67-72, 2019, (Conference Paper).

[24] K. Amara, A. Fekik, D. Hocine, M.L. Bakir, "Improved performance of a PV solar panel with adaptive neuro fuzzy inference system ANFIS based MPPT", 7th International Conference on Renewable Energy Research and Applications (ICRERA). IEEE, 2018. (Conference Paper).

[25] M. Eslami, H. Shareef, A. Mohamed, M. Khajehzadeh, "PSS and TCSC damping controller coordinated design using GSA", Energy Procedia, Vol. 14, pp. 763-769, 2012, (Article).

[26] T. Niknam, F. Golestaneh, A. Malekpour, "Probabilistic energy and operation management of a microgrid containing wind/photovoltaic/fuel cell generation and energy storage devices based on point estimate method and self-adaptive gravitational search algorithm", Energy, Vol. 43, No. 1 ,pp.427-437, 2012, (Article).